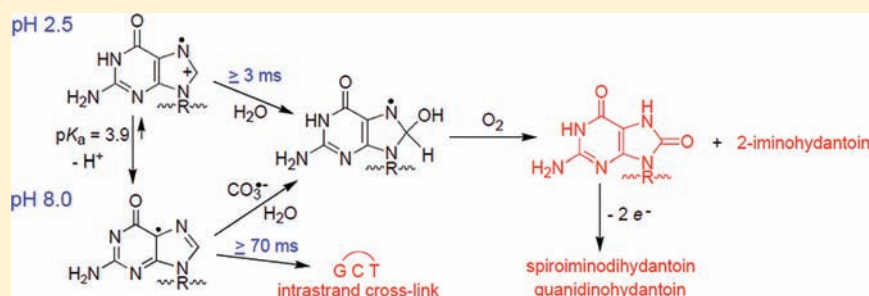


Lifetimes and Reaction Pathways of Guanine Radical Cations and Neutral Guanine Radicals in an Oligonucleotide in Aqueous Solutions

Yekaterina Rokhlenko, Nicholas E. Geacintov, and Vladimir Shafirovich*

Chemistry Department, New York University, 31 Washington Place, New York, New York 10003-5180, United States

S Supporting Information



ABSTRACT: The exposure of guanine in the oligonucleotide 5'-d(TCGCT) to one-electron oxidants leads initially to the formation of the guanine radical cation $G^{\bullet+}$, its deprotonation product $G(-H)^{\bullet}$, and, ultimately, various two- and four-electron oxidation products via pathways that depend on the oxidants and reaction conditions. We utilized single or successive multiple laser pulses (308 nm, 1 Hz rate) to generate the oxidants $CO_3^{\bullet-}$ and $SO_4^{\bullet-}$ (via the photolysis of $S_2O_8^{2-}$ in aqueous solutions in the presence and absence of bicarbonate, respectively) at concentrations/pulse that were ~ 20 -fold lower than the concentration of 5'-d(TCGCT). Time-resolved absorption spectroscopy measurements following single-pulse excitation show that the $G^{\bullet+}$ radical ($pK_a = 3.9$) can be observed only at low pH and is hydrated within 3 ms at pH 2.5, thus forming the two-electron oxidation product 8-oxo-7,8-dihydroguanosine (8-oxoG). At neutral pH, and single pulse excitation, the principal reactive intermediate is $G(-H)^{\bullet}$, which, at best, reacts only slowly with H_2O and lives for ~ 70 ms in the absence of oxidants/other radicals to form base sequence-dependent intrastrand cross-links via the nucleophilic addition of N3-thymidine to C8-guanine (5'-G*CT* and 5'-T*CG*). Alternatively, $G(-H)^{\bullet}$ can be oxidized further by reaction with $CO_3^{\bullet-}$, generating the two-electron oxidation products 8-oxoG (C8 addition) and 5-carboxamido-5-formamido-2-iminohydantoin (2Ih, by C5 addition). The four-electron oxidation products, guanidinohydantoin (Gh) and spiroiminodihydantoin (Sp), appear only after a second (or more) laser pulse. The levels of all products, except 8-oxoG, which remains at a low constant value, increase with the number of laser pulses.

INTRODUCTION

Guanine is the most easily oxidizable nucleic acid base¹ in DNA and is thus the primary target of oxidizing and reactive intermediates, such as free radicals, UV light, and ionizing radiation.² One of the principal one-electron oxidants found in human cells is the carbonate radical anion ($CO_3^{\bullet-}$), which is overproduced at sites of inflammation via spontaneous homolysis of nitrosoperoxycarbonate.³ The primary product of one-electron abstraction from guanine is the guanine radical cation ($G^{\bullet+}$).⁴ The further chemical transformations of this electrophilic intermediate yield a wide spectrum of stable base modifications, which can be considered as products of multielectron oxidation (e.g., 2, 4, and 6 electron oxidation) of guanine,⁵ some of which are depicted in Figure 1. However, the impact of the concentrations of oxidants relative to the guanine substrate concentrations on the distributions of two- or more electron stable oxidation products is poorly understood. In cellular DNA, oxidatively generated guanine lesions occur at levels of the order of one per \sim million guanines.⁶ These low levels of oxidized lesions pose difficulties for the design of in vitro model experiments for gaining deeper understanding of the different

oxidation pathways leading to the products depicted in Figure 1, since the concentrations of oxidants are often in excess of the DNA for assuring the accurate detection and quantification of the guanine lesions formed. These conditions tend to favor the formation of multielectron oxidation products.^{2,5} We developed a new approach to study pathways of oxidation based on the controlled injection of known and relatively low quantities of free radical oxidants by a single or by a train of laser pulses. Both HPLC and mass spectrometry methods were used to investigate the relationships between two- and four-electron guanine oxidation products in the 5'-d(TCGCT) oligonucleotide model system. The concentrations of oxidizing radicals were measured directly by transient absorption spectroscopy and maintained at levels ~ 20 -fold lower than the concentrations of 5'-d(TCGCT) in order to minimize the formation of multielectron oxidation products.

Photochemical methods were utilized to generate the carbonate radical anions or sulfate radical anions as the oxidants.^{7–11}

Received: January 5, 2012

Published: February 13, 2012

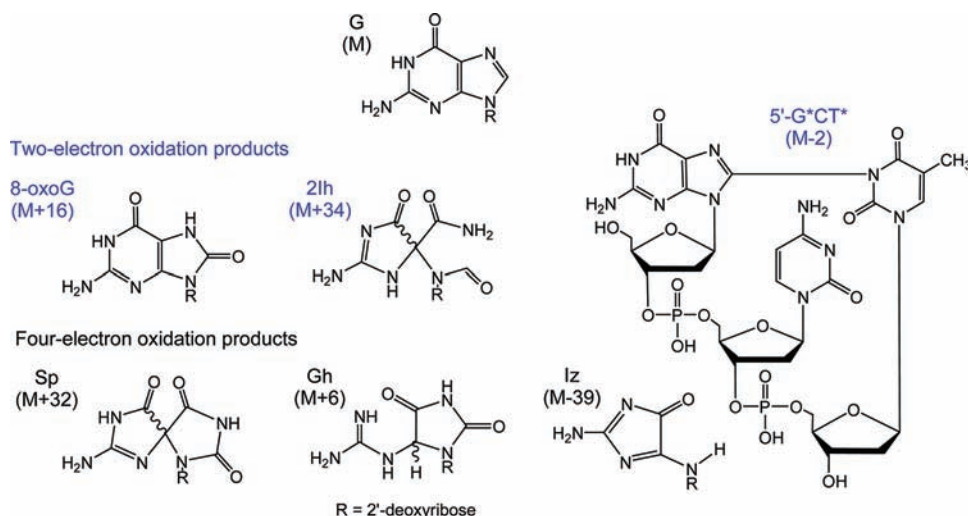


Figure 1. Oxidatively generated guanine lesions.^{2,5,13} 2'-Deoxyribonucleosides of 8-oxo-7,8-dihydroguanosine (8-oxoG), diastereomeric 5-carboxamido-5-formamido-2-iminohydantoin (2Ih), and intrastrand cross-link in which the C8-atom of guanine is covalently linked to the N3-atom of thymidine (5'-G*CT*) are products of two-electron oxidation, whereas guanidinohydantoin (Gh), diastereomeric spiroiminodihydantoin (Sp), and 2,5-diamino-4H-imidazolone (Iz) are products of four-electron oxidation; the masses of these lesions, relative to the mass of G (M), are shown in parentheses.

The former is a mild oxidant with the reduction potential¹² of $E^\circ = 1.59$ V vs NHE that selectively oxidizes guanine in DNA by one-electron mechanisms, thus leading to the formation of a wide spectrum of oxidation products.^{8–11} The sulfate radical anion is a significantly stronger oxidant ($E^\circ = 2.43$ V vs NHE).¹² This reactive intermediate was used to oxidize guanine in 5'-d(TCGCT) at acidic pH values, since the carbonate radical anion cannot be generated at low pH.

We show here that the guanine radical cation generated by the one-electron oxidation of guanine, manifests itself on microsecond time scales only under acidic pH; its lifetime of ~ 3 ms in aqueous solution at pH 2.5 is governed by a hydration mechanism that produces 8-oxo-7,8-dihydroguanosine (8-oxoG). In contrast, at pH values ≥ 7 , only the deprotonation product of $G^{\bullet+}$, the neutral guanine radical, $G(-H)^{\bullet}$, with a lifetime of ~ 70 ms at pH 8, is evident. This intermediate is transformed by various reaction pathways to the different end-products shown in Figure 1. We propose mechanisms of formation and report the proportions of the products formed as a function of the number of successive laser pulses (308 nm, ~ 12 ns duration, 1 Hz repetition rate).

EXPERIMENTAL METHODS

Materials. All chemicals (analytical grade) were used as received. The 5'-d(TCGCT) was purchased from Integrated DNA Technologies (Coralville, IA) and 5'-d(TC[8-oxoG]CT) from Bio-Synthesis (Lewisville, TX). Both oligonucleotides were purified and desalted using reversed-phase HPLC. The integrity of the oligonucleotides was confirmed by MALDI-TOF/MS analysis.

Laser Pulse Photolysis. The kinetics of oxidative reactions initiated by $CO_3^{\bullet-}$ or $SO_4^{\bullet-}$ radicals were monitored directly using a fully computerized kinetic spectrometer system (~ 7 ns response time) described elsewhere.¹⁴ Briefly, an individual single laser pulse selected by an electromagnetic shutter from a train of 308 nm XeCl excimer laser pulses (~ 12 ns, 60 mJ/pulse/cm², 1 Hz) was directed through a rectangular aperture (0.3×1.0 cm) into an 80 μ L sample solution (87 μ M oligonucleotide, 10 mM $Na_2S_2O_8$, and 300 mM $NaHCO_3$ adjusted to pH 8.0 by NaH_2PO_4) in a 0.2×1.0 cm quartz cell. The transient absorbance was probed along a 1 cm optical path by a light beam (75 W xenon arc lamp) oriented perpendicular to the laser beam. The signal was detected with a Hamamatsu 928 photomultiplier

tube and recorded by a Tektronix TDS 5052 oscilloscope operating in its high resolution mode that provides a satisfactory signal/noise ratio after a single laser pulse. The rate constants were determined by least-squares fits of the appropriate kinetic equations to the experimentally measured transient absorption profiles as described in detail elsewhere.⁸ The values reported are averages of five independent measurements. Kinetic modeling was carried out using the INTKIN software developed at the Brookhaven National Laboratory by H. A. Schwarz. The Numerical Integration method used in this program is the DVODE package written by P. N. Brown and A. C. Hindmarsh, Lawrence Livermore National Laboratory, and G. D. Byrne, Exxon Research and Engineering Co.

HPLC Isolation of Oxidatively Generated Oligonucleotide Adducts. After laser pulse irradiation, the samples were immediately subjected to reversed-phase HPLC analysis. The oxidatively modified oligonucleotides were isolated on an analytical (150 \times 4 mm i.d.) ACE C18 (3 μ m, 100 Å) column (MAC-MOD Analytical, Chadd Ford, PA), using a 3–8% linear gradient of acetonitrile in solvent containing 50 mM triethylammonium acetate (TEAA) and 5% acetonitrile for 60 min at a flow rate of 1 mL/min. The products formed in minor quantities were collected after multiple HPLC injections and combined. The HPLC fractions containing the isolated oligonucleotide adducts were thoroughly dried under vacuum to remove most of the TEAA, dissolved in water, and subjected to MALDI-TOF/MS analysis.

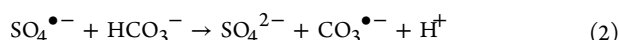
Mass Spectrometry. The MALDI-TOF mass spectra were recorded using a Bruker Daltonics ultrafleXtreme Instrument. In the negative mode, the matrix was a 2:1 mixture of 2',4',6'-trihydroxyacetophenone methanol solution (30 mg/mL) and ammonium citrate aqueous solution (100 mg/mL, whereas in the positive mode, the matrix was a 2,5-dihydroxybenzoic acid (DHB) with concentration 50 mg/mL in 0.1% trifluoroacetic acid (TFA) solution containing 30% acetonitrile and 10 mg/mL of ammonium phosphate.

Generation of Carbonate and Sulfate Radical Anions. Sulfate radicals, $SO_4^{\bullet-}$, were generated by the photodissociation of peroxodisulfate anions, $S_2O_8^{2-}$ (10 mM) induced by single nanosecond 308 nm XeCl excimer laser pulses:



The photodissociation of the peroxodisulfate anions is rapid, and thus, all sulfate radicals are generated within the ~ 12 ns laser pulse duration. If bicarbonate is also present and in excess (300 mM HCO_3^-), the sulfate radicals will decay predominantly and rapidly by

oxidizing bicarbonate, thus resulting in the formation of $\text{CO}_3^{\bullet-}$ radicals, a reaction which is complete within 3 μs after the actinic laser pulse.^{7,8} The observed transient absorbance in the millisecond time range with a maximum at 600 nm is assigned to $\text{CO}_3^{\bullet-}$ radicals produced by the one-electron oxidation of HCO_3^- by $\text{SO}_4^{\bullet-}$ radicals:



that occurs with the rate constant $k_2 = 4.6 \times 10^6 \text{ M}^{-1} \text{ s}^{-1}$.^{7,8} This reaction was used for the generation of $\text{CO}_3^{\bullet-}$ radicals at $\text{pH} \geq 7$; the decomposition of bicarbonate with the formation of carbon dioxide,¹⁵ $\text{pK}(\text{CO}_2, \text{H}_2\text{O}/\text{HCO}_3^-, \text{H}^+) = 6.35$ at 25 °C, suppresses the generation of $\text{CO}_3^{\bullet-}$ radicals at $\text{pH} < 7$, because CO_2 is not oxidized by $\text{SO}_4^{\bullet-}$ radical.¹⁶

RESULTS

Overview. The carbonate radical anion was utilized as the oxidizing species at $\text{pH} \geq 7$, and the sulfate radical at acidic pH. Therefore, we investigated the reactivities of $\text{G}^{\bullet+}$ ($\text{pK}_a = 3.9$)⁴ and the neutral $\text{G}(\text{-H})^{\bullet}$ radical in the oligonucleotide 5'-d(TCGCT) at $\text{pH} 2.5$ and $\text{pH} \geq 7$, respectively. At the low concentrations of $\text{CO}_3^{\bullet-}$ or $\text{SO}_4^{\bullet-}$ radicals generated by individual laser pulses ($[\text{CO}_3^{\bullet-}]$ or $[\text{SO}_4^{\bullet-}] \ll [5\text{'-d(TCGCT)}]$), single-laser pulse excitation was limited to a single initial electron transfer reaction that yielded either $\text{G}(\text{-H})^{\bullet}$ or $\text{G}^{\bullet+}$. Furthermore, the one-second spacing of laser pulses in our multiple laser pulse studies ensured that neither the $\text{CO}_3^{\bullet-}$ nor $\text{SO}_4^{\bullet-}$ radicals survived from pulse-to-pulse.

Single laser pulses produced only the two-electron oxidation products: the $\text{G}^{\bullet+}\text{CT}^{\bullet}$ intrastrand cross-link in which the C8-atom of guanine is covalently linked to the N3-atom of thymidine, the well-known 8-oxo-7,8-dihydroguanine, and the diastereomeric 5-carboxamido-5-formamido-2-iminohydantoin (2Ih) lesions recently described by Gold^{17,18} and Burrows^{5,19} and co-workers (Figure 1). In multiple laser pulse experiments, the diastereomeric spiroiminodihydantoin (Sp), guanidinohydantoin (Gh), and 2,5-diamino-4H-imidazolone (Iz), which are products of four-electron oxidation of guanine (Figure 1), are also formed.

Effect of the Number of Laser Pulses on the Formation of Guanine Lesions. The sample solutions containing 87 μM 5'-d(TCGCT), 10 mM $\text{Na}_2\text{S}_2\text{O}_8$, and 300 mM NaHCO_3 were irradiated by defined numbers of successive 308 nm XeCl excimer laser pulses, and the oxidatively generated products were analyzed by reversed-phase HPLC. Typical reversed-phase chromatograms of the irradiated sample solutions after exposure to 1, 3, or 10 laser pulses are shown in Figure 2. It is evident that the amounts and the relative distributions of guanine oxidation products in the oligonucleotide 5'-d(TCGCT) depend on the number of pulses and that there are no products in the unirradiated sample (Figure 2).

In each individual experiment, the end products were separated by reversed-phase HPLC methods and identified by MALDI-TOF/MS analysis and by coelution with authentic standards synthesized by laser flash and continuous illumination photochemical methods developed in our group and described in detail elsewhere.⁸⁻¹¹ We found that the major products are modified oligonucleotides containing oxidatively modified guanine bases. The adducts derived from two-electron oxidations of guanine include 5'-d(TCG*CT*), 5'-d(TC[8-oxoG]CT), and the diastereomeric 5'-d(TC[2Ih]CT) eluted at 13.5 (1), 28.0 (8), and 17.0–17.8 (5, 6) min, respectively (Figure 2). In turn, the adducts produced by four-electron oxidation of guanine include the diastereomeric 5'-d(TC[Sp]CT), 5'-d(TC[Gh]CT), and 5'-d(TC[Iz]CT) eluting at

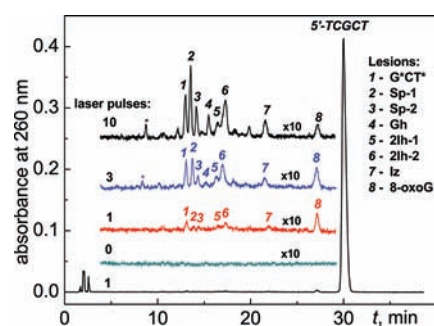


Figure 2. Oxidatively generated end-products detected after excitation with different numbers of 308 nm nanosecond laser pulses. The irradiated 80 μL solution aliquots were air-equilibrated buffer solutions ($\text{pH} 8.0$) containing 87 μM 5'-d(TCGCT), 10 mM $\text{Na}_2\text{S}_2\text{O}_8$, and 300 mM NaHCO_3 . Reversed-phase HPLC elution conditions (detection of products at 260 nm): 3–8% gradient of acetonitrile in aqueous solvent containing 50 mM triethylammonium acetate and 5% acetonitrile for 60 min at a flow rate of 1 mL/min. The adduct marked by the asterisk (*) has the same mass as the $\text{G}^{\bullet+}\text{CT}^{\bullet}$ adduct (M-2, labeled 1 in the figure) and was assigned to the analogous cross-linked 5'-d(T*CG*CT) product.¹⁰

14.0–14.7 (2, 3), 16.0 (6), and 22.2 (7) min, respectively (Figure 2). We also observed the 5'-d(T*CG*CT) cross-linked adduct that elutes at 8.0 min (denoted by an asterisk (*) in Figure 2), which is typically formed in smaller quantities than 5'-d(TCG*CT*) product 1.¹⁰

The yields of oligonucleotide adducts as a function of the number of laser pulses are shown in Figure 3.

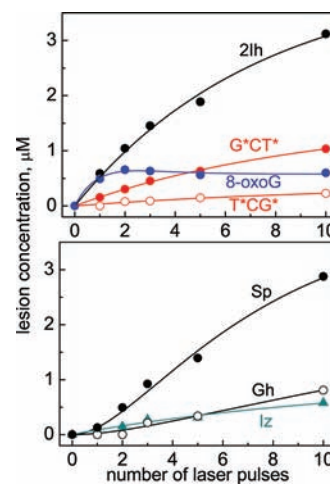


Figure 3. Dependence of the yields of the $\text{G}^{\bullet+}\text{CT}^{\bullet}$, $\text{T}^{\bullet}\text{CG}^{\bullet}$, 8-oxoG, 2Ih, Sp, Gh, and Iz oligonucleotide adducts on the number of successive 308 nm laser pulses in air-equilibrated buffer solutions ($\text{pH} 8.0$) containing 87 μM 5'-d(TCGCT), 10 mM $\text{Na}_2\text{S}_2\text{O}_8$, and 300 mM NaHCO_3 . The modified oligonucleotide yields were estimated by integrating the areas under each elution band in the HPLC profiles and utilizing the molar absorptivities of the oligonucleotide adducts at 260 nm.

Increasing the number of laser pulses induces a monotonic rise in the yields of the 5'-d(TCG*CT*) and 5'-d(TC[2Ih]CT) adducts. However, the yield of the 5'-d(TC[8-oxoG]CT) product attains a maximum value after two laser pulses and slowly decreases with increasing number of pulses. The yields of the Sp- and Gh-containing oligonucleotide products based on the number of laser pulses are quite different; the yields are

negligible after the first laser pulse and then gradually rise after the second pulse. Overall, these results suggest that a single laser pulse generates 5'-d(TCG*CT*), 5'-d(TC[2Ih]CT), and 5'-d(TC[8-oxoG]CT) adducts. The 8-oxoG in the latter is more reactive than guanine in the parent 5'-d(TCGCT), and thus, 5'-d(TC[8-oxoG]CT) is further oxidized to yield 5'-d(TC[Sp]CT) and 5'-d(TC[Gh]CT). These reactions prevent the growth of the 5'-d(TC[8-oxoG]CT) product levels with increasing numbers of laser pulses. In agreement with this mechanism, excitation of sample solutions containing only an authentic 5'-d(TC[8-oxoG]CT) sample in a 10 mM Na₂S₂O₈ and 300 mM NaHCO₃ solution generates 5'-d(TC[Sp]CT) and 5'-d(TC[Gh]CT) adducts after irradiation with a single laser pulse. Note, that the formation of G*CT* cross-links is base sequence-dependent because the yields of 5'-G*CT* are higher than the yields of the 5'-T*CG* cross-linked products (Figure 3).

Formation of Imidazolone Lesions. Reversed-phase HPLC analysis of the oxidation products showed that oligonucleotides containing imidazolone lesions (7) are also formed (Figure 2). Increasing the number of laser pulses induces a monotonic growth of the yields of the 5'-d(TC[Iz]CT) adducts (Figure 3B). The major pathway of formation of Iz lesions is the combination reaction of G(-H)[•] radicals with superoxide, O₂^{•-}, and peroxy radicals, RO₂[•].^{20,21} Here, we propose that side reactions of SO₄^{•-} radicals generate C-centered alkyl radicals of pyrimidine bases (T and C) and 2-deoxyribose,^{22,23} which in the presence of oxygen can serve as a source of RO₂[•]/O₂^{•-} radicals.^{24,25}

Comparisons of 8-oxoG and G*CT* Product Yields at Different pH Values Generated by Carbonate or Sulfate Radical Anions. The primary molecular products of guanine oxidation are products of two-electron oxidation, which can form by two alternative pathways: (1) addition of nucleophiles to guanine radicals followed by one-electron oxidation of radical adducts, and (2) combination of guanine radicals with other free radicals.^{2,13} The first pathway suggests a correlation of the product yields with the solution pH, which can affect the nucleophilicity/electrophilicity of the reaction partners. In turn, the reactivities of radicals (CO₃^{•-} or SO₄^{•-}) can affect product formation via radical combination. The yields of 5'-d(TCG*CT*) adducts generated by CO₃^{•-} radicals injected by a single laser pulse excitation gradually increase with increasing pH from 7 to 9 (Figure 4), which correlates with

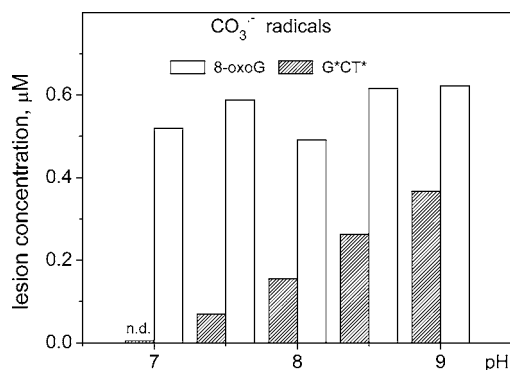


Figure 4. Effect of pH on the generation of 5'-d(TCG*CT*) and 5'-d(TC[8-oxoG]CT) induced by CO₃^{•-} radicals produced by a single laser pulse irradiation of an 87 μM 5'-d(TCGCT), 10 mM Na₂S₂O₈, and 300 mM NaHCO₃ solution. The G*CT* adduct was not detected (n.d.) at pH 7.0.

enhancement of the thymine nucleophilicity.¹¹ However, the yield of 5'-d(TC[8-oxoG]CT) does not change significantly and remains practically unchanged in this pH range, in agreement with the radical combination mechanism.⁹

In contrast, when the solution composition was altered to produce only sulfate radical anions by single pulse irradiation experiments of a solution without bicarbonate anions, no 5'-d(TC[8-oxoG]CT) products were detected in the pH 7–8 range (Figure 5).

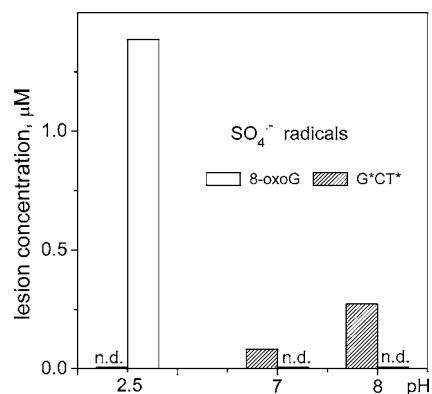


Figure 5. Effect of pH on the generation of 5'-d(TCG*CT*) and 5'-d(TC[8-oxoG]CT) produced by SO₄^{•-} radicals. The latter were generated by irradiation of an 87 μM 5'-d(TCGCT), 10 mM Na₂S₂O₈ solution by a single laser pulse. The G*CT* and 8-oxoG adducts were not detected (n.d.) at pH 2.5, whereas 8-oxoG adducts were not detected at pH 7–8.

The oxidation of 5'-d(TCGCT) by SO₄^{•-} radicals can generate 8-oxoG lesions *only* in slightly acidic solutions (pH 2.5), where the guanine radicals G^{•+} (pK_a = 3.9) exist in the cationic form and do not deprotonate to form neutral radicals, G(-H)[•].⁴ However, the 5'-d(TCG*CT*) adducts are not formed in acidic solutions but are generated in neutral solutions (pH 7–8), with yields similar to those observed in the presence of HCO₃⁻ anions, and grow with increasing pH, as demonstrated in Figure 5. These differences in oxidative pathways of guanine oxidation by CO₃^{•-} and SO₄^{•-} radicals account for the difference in the distribution of end-products generated by these radicals with the relative yields summarized in Table 1.

Table 1. Relative Yields (%) of the 5'-d(TCG*CT*) and 5'-d(TC[8-oxoG]CT) Adducts Produced by CO₃^{•-} and SO₄^{•-} Radicals^a

oxidant	8-oxoG	G*CT*
CO ₃ ^{•-}	0.57 (pH 8.0)	0.31 (pH 8.0)
SO ₄ ^{•-}	1.60 (pH 2.5)	0.18 (pH 8.0)
SO ₄ ^{•-}	≤0.01 (pH 8.0)	≤0.01 (pH 2.5)

^aThe latter were generated by irradiation of an 87 μM 5'-d(TCGCT), 10 mM Na₂S₂O₈ solution (pH 2.5 or 8.0) by a single laser pulse.

Kinetics of Guanine Radical Formation and Decay.

Further information about oxidative reaction pathways can be obtained by examining the kinetics of some of the reactive intermediates observed by irradiating solutions containing 87 μM 5'-d(TCGCT), 10 mM Na₂S₂O₈, and 300 mM NaHCO₃ in air-equilibrated buffer solutions. The CO₃^{•-} radicals exhibit a characteristic transient absorption band at 600 nm with the

molar extinction coefficient²⁶ $\epsilon = 1.97 \times 10^3 \text{ M}^{-1} \text{ cm}^{-1}$, which is greater than the ϵ values of the other free radicals at this wavelength (inset in Figure 6A).^{7,8}

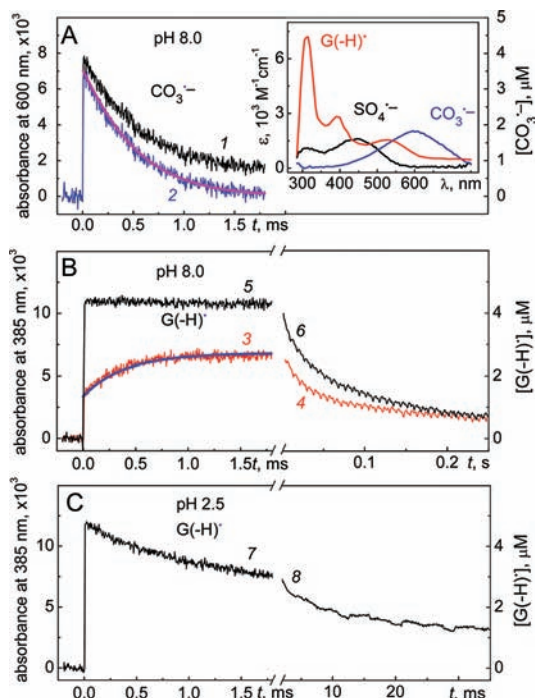
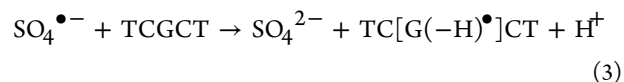


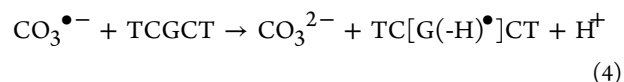
Figure 6. Kinetics of free radical reactions induced by a 308 nm nanosecond single laser pulse excitation of air-equilibrated buffer solutions containing $87 \mu\text{M}$ 5'-d(TCGCT), 10 mM $\text{Na}_2\text{S}_2\text{O}_8$, and 300 mM NaHCO_3 at different values of pH. (A) Transient absorbance recorded at 600 nm at pH 8.0 (black trace 1). The blue trace 2 was determined by subtraction of the $\text{G}(-\text{H})^\bullet$ absorbance at each time point from the black trace 1. Thus, trace 2 represents the decay of $\text{CO}_3^{\bullet-}$ radicals. The inset depicts the transient absorption spectra of $\text{CO}_3^{\bullet-}$, $\text{SO}_4^{\bullet-}$, and $\text{G}(-\text{H})^\bullet$ radicals showing that there is some overlap in the absorption spectra of $\text{CO}_3^{\bullet-}$ and $\text{G}(-\text{H})^\bullet$ radicals at 600 nm . (B) Transient absorption profiles recorded at 385 nm and attributed to the formation and decay of $\text{G}(-\text{H})^\bullet$ radicals in buffer solution containing 300 mM NaHCO_3 , pH 8.0 (red traces 3 and 4, oxidation produced by $\text{CO}_3^{\bullet-}$ radicals), and without NaHCO_3 (black traces 5 and 6, oxidation generated by $\text{SO}_4^{\bullet-}$ radicals only). (C) Formation and decay of the $\text{G}(-\text{H})^\bullet$ radicals generated by $\text{SO}_4^{\bullet-}$ radicals (black traces 7 and 8) at pH 2.5 (in the absence of NaHCO_3). The time courses of formation and decay of $\text{CO}_3^{\bullet-}$ radicals (magenta, solid curve superimposed on the experimental data shown in blue, curve 2, panel A) and $\text{G}(-\text{H})^\bullet$ radicals (blue, solid curve superimposed on the experimental data shown in red, curve 3, panel B) involved in reactions 4–6 (see text) were simulated with the following best-fit rate constants, $k_4 = 1.5 \times 10^7$, $k_{5a} = 1.4 \times 10^8$, $k_{5b} = 1.6 \times 10^8$, and $k_6 = 3.0 \times 10^8 \text{ M}^{-1} \text{ s}^{-1}$, and the initial concentrations, $[\text{CO}_3^{\bullet-}]_0 = 3.60 \mu\text{M}$ and $[\text{G}(-\text{H})^\bullet]_0 = 1.25 \mu\text{M}$.

The transient absorption spectrum of $\text{G}(-\text{H})^\bullet$ radicals shows a narrow absorption band at 315 nm and two less intense bands near 390 and 510 nm (inset in Figure 6A).^{4,27} To exclude photolysis of the sample solution by the probe light, we utilized a 360 nm cutoff filter and monitored the formation and decay of $\text{G}(-\text{H})^\bullet$ radicals at 385 nm . At this wavelength, the extinction coefficient of $\text{G}(-\text{H})^\bullet$ radicals⁴ ($\epsilon = 2.7 \times 10^3 \text{ M}^{-1} \text{ cm}^{-1}$) is greater than the molecular absorptivities of $\text{SO}_4^{\bullet-}$ radicals²⁸ ($\epsilon = 1.6 \times 10^3 \text{ M}^{-1} \text{ cm}^{-1}$) and of $\text{CO}_3^{\bullet-}$ radicals (negligible at 385 nm).

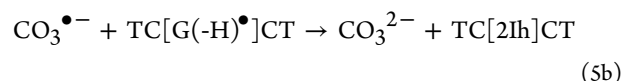
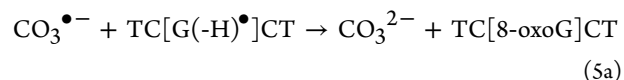
At pH 8.0, the lifetime of $\text{CO}_3^{\bullet-}$ radicals is reduced from $\sim 7.7 \text{ ms}$ in the absence of 5'-d(TCGCT) to $\sim 0.5 \text{ ms}$ in the presence of $87 \mu\text{M}$ 5'-d(TCGCT) (blue trace 2, Figure 6A). The growth of the transient absorbance at 385 nm associated with the $\text{G}(-\text{H})^\bullet$ radicals is characterized by two kinetic components (red trace 3, Figure 6B). The first and fast component, which was not time-resolved in the experiment shown in Figure 6B, is assigned to the direct oxidation of 5'-d(TCGCT) by $\text{SO}_4^{\bullet-}$ radicals:



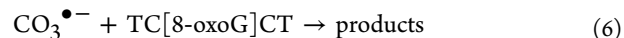
Reaction 3 contributes to the formation of $\text{G}(-\text{H})^\bullet$ radicals even at high concentrations of HCO_3^- (300 mM), because the values of k_3 are typically very high, $(2-3) \times 10^9 \text{ M}^{-1} \text{ s}^{-1}$, and are close to the diffusion-controlled limit.^{7,8,29} The second millisecond component ($\sim 0.5 \text{ ms}$) is correlated with the decay of $\text{CO}_3^{\bullet-}$ radicals (blue trace 2, Figure 6A) and, hence, is assigned to oxidation of 5'-d(TCGCT) by $\text{CO}_3^{\bullet-}$ radicals:



However, the yield of $\text{G}(-\text{H})^\bullet$ radicals formed in this process ($1.28 \mu\text{M}$, calculated as a difference of the yields at 1.8 and 0.01 ms) is significantly less than the yield of $\text{CO}_3^{\bullet-}$ radicals ($\sim 3.60 \mu\text{M}$) in reaction 2 (blue trace 2, Figure 6A). To explain this difference between the expected and observed yields of $\text{G}(-\text{H})^\bullet$ radicals in $\text{TC}[\text{G}(-\text{H})^\bullet]\text{CT}$, we propose that the $\text{G}(-\text{H})^\bullet$ radicals derived from reactions 3 and 4 are rapidly oxidized by $\text{CO}_3^{\bullet-}$ radicals to form the two-electron oxidation products (8-oxoG and 2Ih):



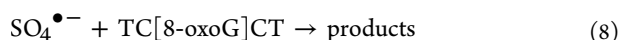
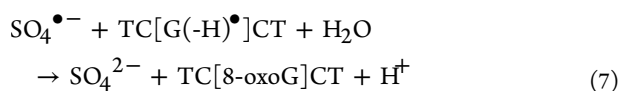
Indeed, the simple kinetic scheme, which includes reactions 4, 5a, and 5b discussed above, as well as reaction 6 describing the further oxidation of 5'-d(TC[8-oxoG]CT) by $\text{CO}_3^{\bullet-}$ radicals,



can account for the kinetics and yields of $\text{G}(-\text{H})^\bullet$ radicals in the presence of HCO_3^- anions. The simulated kinetic curves describing the decay of $\text{CO}_3^{\bullet-}$ radicals (magenta curve in Figure 6A) and the formation $\text{G}(-\text{H})^\bullet$ radicals (blue curve in Figure 6B) agree with the experimental kinetic profiles (blue trace 2 in Figure 6A and red trace 3 in Figure 6B, respectively). This scheme also predicts that the yield of 8-oxoG lesions should attain a relatively constant value after several laser flashes (Figure S1 in the Supporting Information) as observed in the experiment (Figure 3).

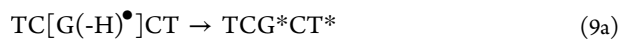
Upon excitation with a single laser pulse and in the absence of HCO_3^- anions, $\text{G}(-\text{H})^\bullet$ radicals are formed via oxidation by $\text{SO}_4^{\bullet-}$ radicals (reaction 3) within $10 \mu\text{s}$ following the 12 ns actinic laser pulse. This is evident from the rapid rise in the $\text{G}(-\text{H})^\bullet$ absorbance measured at 385 nm (black trace 7, Figure 6B). A simple kinetic scheme, based on reaction 3 (generation of $\text{G}(-\text{H})^\bullet$ radicals), reaction 7 (oxidation of $\text{G}(-\text{H})^\bullet$ radicals to

form 8-oxoG lesions), and reaction 8 (oxidation of 8-oxoG) was developed:



This kinetic scheme predicts that the value of the rate constant k_7 should be at the level of $\sim 6 \times 10^{10} \text{ M}^{-1} \text{ s}^{-1}$ (Figure S2 in the Supporting Information) to achieve yields of 8-oxoG that are comparable to those generated by $\text{CO}_3^{\bullet-}$ radicals (Figure 3). However, this value of k_7 is unrealistic because it is one order of magnitude greater than the diffusion-controlled limit. Therefore, it is not surprising that we did not observe any 8-oxoG lesions upon oxidation of 5'-d(TCGCT) with $\text{SO}_4^{\bullet-}$ radicals after a single laser pulse excitation in the absence of HCO_3^- anions (Figure 5).

In air-equilibrated buffer solutions (pH 8.0), the $\text{G}(-\text{H})^{\bullet}$ radicals decay relatively slowly with characteristic lifetimes of $\sim 0.07 \text{ s}$, which are not affected by the presence of oxidants ($\text{CO}_3^{\bullet-}$, red trace 4, or $\text{SO}_4^{\bullet-}$, black trace 6), as shown in Figure 6B. The value of the rate constant $k_9 \sim 15 \text{ s}^{-1}$, defined by the reactions (pH 8.0),



can be estimated from the lifetimes of $\text{G}(-\text{H})^{\bullet}$ radicals; the value of this constant is an upper limit that defines the rate of formation of the cross-linked products after a single laser pulse excitation (Figure 5).

In acid solutions, only $\text{SO}_4^{\bullet-}$ radicals can be used as oxidants, since HCO_3^- anions (precursors of $\text{CO}_3^{\bullet-}$ radicals) decompose to CO_2 and H_2O below pH 7. At pH 2.5, the formation of guanine radicals is complete within 10 μs , and the yield of $\text{G}(-\text{H})^{\bullet}$ radicals (black trace 7, Figure 6C) is close to the yields at pH 8.0 (black trace 5, Figure 6B). At pH 2.5, the guanine radicals exist in the form of the radical cations,⁴ $\text{G}^{\bullet+}$ ($\text{p}K_a = 3.9$), and decay with the characteristic lifetime of $\sim 3 \text{ ms}$ or rate constant $k_{10} \sim 3.3 \times 10^2 \text{ s}^{-1}$. The latter can be considered as the upper limit for the formation of 8-oxoG lesions according to the following reaction:



Consistent with this mechanism, the 8-oxoG lesions were detected by reversed-phase HPLC after a single laser pulse excitation of the sample solutions (Figure 5). The G^*CT^* cross-links were not detected; the lifetime of $\text{G}^{\bullet+}$ is too short at pH 2.5 due to hydration, which limits the lifetime of $\text{G}^{\bullet+}$ to $\sim 3 \text{ ms}$, and reaction 9 occurring with the characteristic time of $\sim 70 \text{ ms}$ cannot compete with reaction 10.

DISCUSSION

In this work, the one-electron oxidation of guanine bases in DNA sequences was initiated by $\text{CO}_3^{\bullet-}$ or $\text{SO}_4^{\bullet-}$ radicals produced by a single laser pulse excitation. The different reaction pathways established are summarized in Figure 7.

In agreement with these constraints, guanine radicals generated by $\text{SO}_4^{\bullet-}$ radicals at pH 2.5 ($\text{p}K_a = 3.9$) exist mostly in the cation form, $\text{G}^{\bullet+}$. Hydration of $\text{G}^{\bullet+}$ radicals results in the formation of 8-hydroxy-7,8-dehydroguanyl radicals (8-HO- G^{\bullet}), which are identical to the radical adducts derived

from addition of hydroxyl radicals to the C8 position of guanine.² The latter are reducing and are rapidly oxidized by weak oxidants such as oxygen, methylviologen, and 1,4-benzoquinone to form 8-oxoG lesions.³⁰ The upper limit of the hydration rate constant, $k_{10} \sim 3.3 \times 10^2 \text{ s}^{-1}$, was estimated from the decay of $\text{G}^{\bullet+}$ radicals recorded at 385 nm and at pH 2.5 (traces 7 and 8, Figure 6C). This is the first estimate of this rate constant by direct spectroscopic measurements; it is 2 orders of magnitude smaller than the rate constant of $6 \times 10^4 \text{ s}^{-1}$ obtained by computer modeling of the distributions of alkali-labile guanine lesions in DNA.³¹

The kinetics of the buildup of the $\text{G}(-\text{H})^{\bullet}$ absorption band at 625 nm band was utilized to measure the deprotonation rate constant of $\text{G}^{\bullet+}$ radicals, which varies from $1.8 \times 10^7 \text{ s}^{-1}$ for the free nucleoside to $\geq 3 \times 10^6 \text{ s}^{-1}$ in double-stranded DNA.^{32,33} The deprotonation of $\text{G}^{\bullet+}$ has been described in terms of a release of the N1 proton and the formation of the $\text{G}(\text{N1}-\text{H})^{\bullet}$ tautomer.³⁴ On the basis of EPR studies in aqueous solutions (pH ≤ 3) at room temperature, coupled with a theoretical study, it was concluded that the $\text{G}^{\bullet+}$ radical is protonated at N1 and is indeed deprotonated by the loss of the proton at N1 to form the $\text{G}(\text{N1}-\text{H})^{\bullet}$ neutral radical at pH > 4 .³⁵ Extensive DFT calculations of various tautomeric forms of $\text{G}(-\text{H})^{\bullet}$ confirm that in aqueous solution $\text{G}(\text{N1}-\text{H})^{\bullet}$ is the most stable form of the neutral guanine radical.³⁶ Here, we propose two different pathways of $\text{G}(-\text{H})^{\bullet}$ radical decay that lead to the 8-oxoG or G^*CT^* lesions that are detected experimentally after irradiation of 5'-d(TCGCT) with a single laser pulse (Figure 7).

The formation of the G^*CT^* cross-links occur via the nucleophilic addition of thymine to the C8 position of the $\text{G}(-\text{H})^{\bullet}$ radical (Figure 7). Increasing the pH facilitates deprotonation of T-N3(H), since its $\text{p}K_a = 9.67$,³⁷ and thus greatly enhances the nucleophilicity of thymine due to the formation of $(\text{T}-\text{N3})^-$. The $\text{G}(\text{C8})-(\text{N3})\text{T}$ radical adduct formed is easily oxidized by oxygen, thus resulting in the formation of the G^*CT^* cross-link. This adduct can also be oxidized by other mild oxidants, such as 1,4-benzoquinone in deoxygenated aqueous solutions.³⁸ This mechanism does not depend on the oxidant ($\text{CO}_3^{\bullet-}$ or $\text{SO}_4^{\bullet-}$ radical) used for the generation of $\text{G}(-\text{H})^{\bullet}$ radicals and can account for a gradual growth of the yields of the G^*CT^* lesions with increasing pH (Figure 5). A similar nucleophilic mechanism was proposed by Perrier et al. for the formation of cross-linked products between guanine in d(TpGpT) and lysine mediated by photoexcited riboflavin in aerated solutions containing the KKK tripeptide.³⁹

The neutral radical, $\text{G}(-\text{H})^{\bullet}$, is a weaker electrophile than the radical cation $\text{G}^{\bullet+}$ and does not react directly with water, which could account for the absence of 8-oxoG observed after single laser pulse excitation (Figures 2 and 5) and continuous UV illumination, as reported earlier.¹⁰ In this work, we demonstrate that $\text{CO}_3^{\bullet-}$ radicals can oxidize $\text{G}(-\text{H})^{\bullet}$ radicals. The rate constant of this reaction, $k_5 = (3.0 \pm 0.5) \times 10^7 \text{ M}^{-1} \text{ s}^{-1}$ was obtained from analysis of the transient absorption profiles monitored by laser flash photolysis (Figure 6). This value of k_5 is similar to the rate constants of the addition of oxyl radicals (e.g., $\text{O}_2^{\bullet-}$, $\bullet\text{NO}_2$) to $\text{G}(-\text{H})^{\bullet}$ radicals.^{20,40} As in the case of other oxyl radicals ($\text{O}_2^{\bullet-}$, $\bullet\text{NO}_2$), the combination of $\text{G}(-\text{H})^{\bullet}$ and $\text{CO}_3^{\bullet-}$ radicals occurs via the addition of $\text{CO}_3^{\bullet-}$ to the C8 and C5 positions of $\text{G}(-\text{H})^{\bullet}$ radicals (Figure 7). The adducts formed, which can be considered as the monoesters of carbonic acid, H_2CO_3 , are unstable and rapidly decompose to form the final products, 8-oxoG and the diastereomeric 2Ih

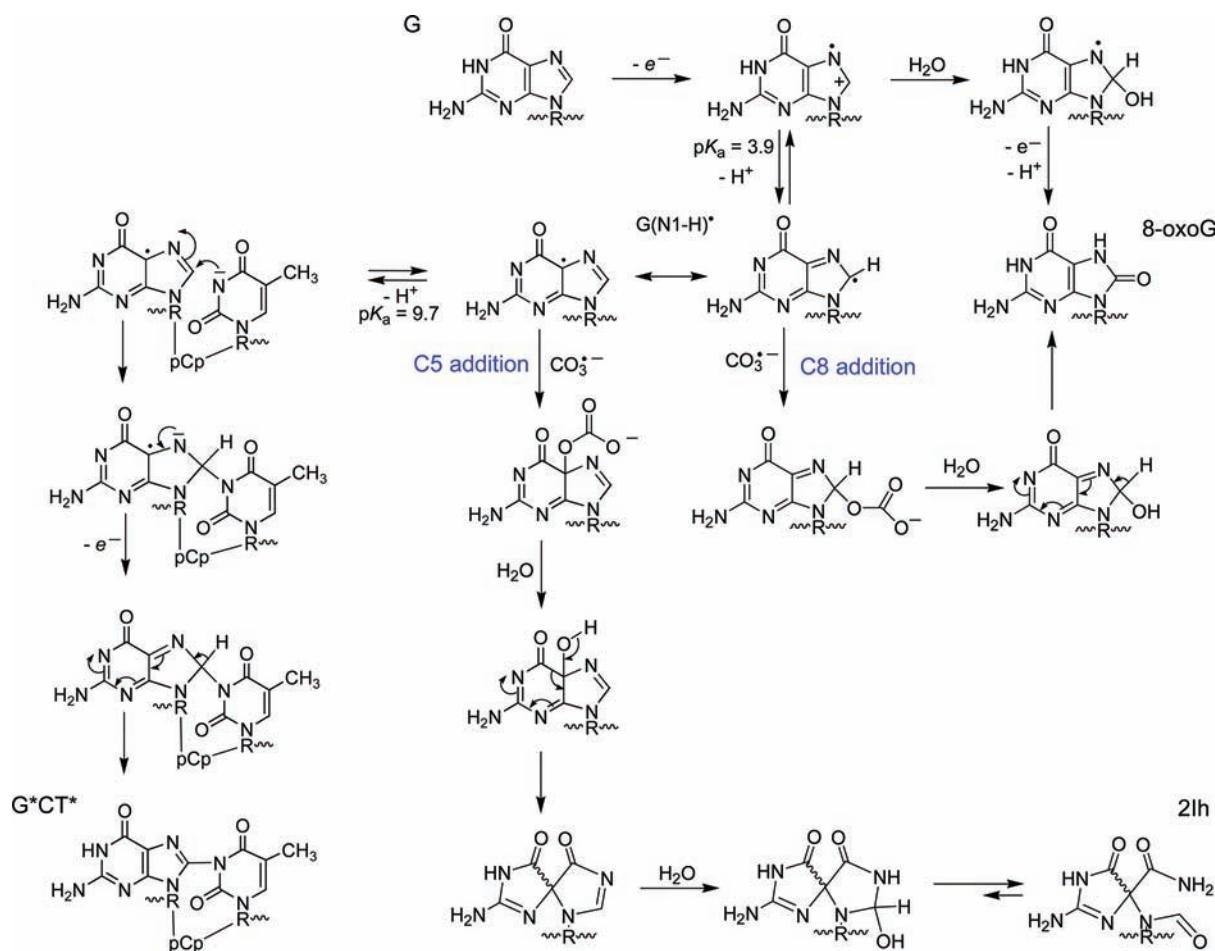


Figure 7. One-electron oxidation of guanine bases in oligonucleotides in a GCT sequence context by CO₃^{•-} or by SO₄^{•-} radicals.

lesions. The partitioning of CO₃^{•-} radical addition to either C5 or C8 of G(-H)[•] can be determined from the ratio of 2lh/8-oxoG lesions, which is ~1.2, detected after a single laser pulse (Figure 3). The DNA secondary structure can affect the ratio of the C5/C8 products. In the case of •NO₂ radicals, the ratio of 5-guanidino-4-imidazolone (C5 addition)/8-nitroguanine (C8 addition) gradually decreases from 3.4 in the model compound, 2',3',5'-tri-*O*-acetylguanosine, to 2.1–2.6 in single-stranded oligodeoxynucleotides, to 0.8–1.1 in double-stranded DNA.⁴¹ Here, this effect is accounted for in terms of the relative accessibilities of the C5 and C8 positions of G(-H)[•] radicals by carbonate radicals and the further transformation of the adducts formed to end-products such as 2lh (C5 addition) or 8-oxoG (C8 addition).

CONCLUSIONS

The one-electron oxidation of guanine bases in single-stranded oligonucleotides in the 5'-...TCGCT... sequence context by CO₃^{•-} and SO₄^{•-} radicals generates guanine radical cations. In neutral solutions, the G^{•+} radicals rapidly deprotonate to form guanine neutral radicals, G(-H)[•]. The transformation of G(-H)[•] radicals to chemical end products occurs by two principal pathways: (i) combination of G(-H)[•] and CO₃^{•-} radicals followed by the formation of 8-oxoG and 2lh lesions, and (ii) nucleophilic addition of thymine bases to G(-H)[•] followed by the formation of 5'-G*CT* and 5'-T*CG* cross-links. The cross-linking reaction is very slow and occurs with the characteristic time of ≥70 ms. In acid solutions (pH 2.5), the

principal pathway of G^{•+} decay is hydration that is followed by the formation of 8-oxoG lesions.² This hydration reaction, estimated from the decay time of the radical cation at pH 2.5, occurs within a characteristic time of ≥3 ms. Under physiological conditions (pH 7–8), the major decay pathway of the G^{•+} radical cation is deprotonation that occurs in double-stranded DNA within 300 ns.^{36,37} The ratio of the hydration/deprotonation rates of G^{•+} estimated from the characteristic times of these reactions suggests that the yields of 8-oxoG formed are ≤0.01% per guanine radical cation generated by the one-electron oxidation mechanism. Such a low efficiency of 8-oxoG formation originating via the G^{•+} pathway is consistent with the lack of observation of 8-oxoG formation in our sulfate radical oxidation experiments at pH 8.0 (Table 1). Furthermore, the long lifetime of the G(-H)[•] radical in neutral aqueous solutions (~70 ms in the absence of other reactive radical intermediates, Figure 6B) is not limited by hydration that would have yielded 8-oxoG at pH 8.0. In the case of cellular DNA, the levels of 8-oxoG lesions are quite small (0.3–4.2 8-oxoG per 10⁶ guanines⁶). However, these low yields may be due to other factors (e.g., low yields of G^{•+} radicals and differences in reaction pathways of these radicals in cellular environments, as well as base excision repair of 8-oxoG lesions).

ASSOCIATED CONTENT

Supporting Information

Simulated kinetics of reactions of CO₃^{•-} and G(-H)[•] radicals, and yields of the 8-oxoG, 2lh, Sp, and Gh molecular products as

a function of the number of laser pulses (Figure S1); simulated kinetics of the $\text{SO}_4^{\bullet-}$ and $\text{G}(\text{-H})^{\bullet}$ radicals and yields of 8-oxoG produced by a single laser pulse excitation (Figure S2). This material is available free of charge via the Internet at <http://pubs.acs.org>.

AUTHOR INFORMATION

Corresponding Author

vs5@nyu.edu

Notes

The authors declare no competing financial interest.

ACKNOWLEDGMENTS

This work was supported by the National Institute of Environmental Health and Sciences (Grant 2 R01 ES 011589-10). Components of this work were conducted in the Shared Instrumentation Facility at NYU that was constructed with support from a Research Facilities Improvement Grant (C06 RR-16572) from the National Center for Research Resources, National Institutes of Health. The acquisition of the MALDI-TOF mass spectrometer was supported by the National Science Foundation (CHE-0958457).

REFERENCES

- (1) Steenken, S.; Jovanovic, S. V. *J. Am. Chem. Soc.* **1997**, *119*, 617–618.
- (2) Cadet, J.; Douki, T.; Ravanat, J. L. *Acc. Chem. Res.* **2008**, *41*, 1075–1083.
- (3) Pacher, P.; Beckman, J. S.; Liaudet, L. *Physiol. Rev.* **2007**, *87*, 315–424.
- (4) Candeias, L. P.; Steenken, S. *J. Am. Chem. Soc.* **1989**, *111*, 1094–1099.
- (5) Fleming, A. M.; Muller, J. G.; Burrows, C. J. *Org. Biomol. Chem.* **2011**, *9*, 3338–3348.
- (6) Collins, A. R.; Cadet, J.; Moller, L.; Poulsen, H. E.; Vina, J. *Arch. Biochem. Biophys.* **2004**, *423*, 57–65.
- (7) Shafirovich, V.; Dourandin, A.; Huang, W.; Geacintov, N. E. *J. Biol. Chem.* **2001**, *276*, 24621–24626.
- (8) Joffe, A.; Geacintov, N. E.; Shafirovich, V. *Chem. Res. Toxicol.* **2003**, *16*, 1528–1538.
- (9) Crean, C.; Geacintov, N. E.; Shafirovich, V. *Angew. Chem., Int. Ed. Engl.* **2005**, *44*, 5057–5060.
- (10) Crean, C.; Uvaydov, Y.; Geacintov, N. E.; Shafirovich, V. *Nucleic Acids Res.* **2008**, *36*, 742–755.
- (11) Crean, C.; Lee, Y. A.; Yun, B. H.; Geacintov, N. E.; Shafirovich, V. *ChemBioChem* **2008**, *9*, 1985–1991.
- (12) Huie, R. E.; Clifton, C. L.; Neta, P. *Radiat. Phys. Chem.* **1991**, *38*, 477–481.
- (13) Shafirovich, V.; Geacintov, N. E. In *Radical and radical ion reactivity in nucleic acid chemistry*; Greenberg, M., Ed.; John Wiley & Sons, Inc.: Hoboken, NJ, 2009; pp 325–355.
- (14) Shafirovich, V.; Dourandin, A.; Huang, W.; Luneva, N. P.; Geacintov, N. E. *J. Phys. Chem. B* **1999**, *103*, 10924–10933.
- (15) Harned, H. C.; Bonner, F. C. *J. Am. Chem. Soc.* **1945**, *67*, 1026–1031.
- (16) Neta, P.; Huie, R. E.; Ross, A. B. *J. Phys. Chem. Ref. Data* **1988**, *17*, 1027–1284.
- (17) Ye, W.; Sangaiah, R.; Degen, D. E.; Gold, A.; Jayaraj, K.; Koshlap, K. M.; Boysen, G.; Williams, J.; Tomer, K. B.; Ball, L. M. *Chem. Res. Toxicol.* **2006**, *19*, 506–510.
- (18) Ye, W.; Sangaiah, R.; Degen, D. E.; Gold, A.; Jayaraj, K.; Koshlap, K. M.; Boysen, G.; Williams, J.; Tomer, K. B.; Mocanu, V.; Dicheva, N.; Parker, C. E.; Schaaper, R. M.; Ball, L. M. *J. Am. Chem. Soc.* **2009**, *131*, 6114–6123.
- (19) Ghude, P.; Schallenberger, M. A.; Fleming, A. M.; Muller, J. G.; Burrows, C. J. *Inorg. Chim. Acta* **2011**, *369*, 240–246.
- (20) Misiaszek, R.; Crean, C.; Joffe, A.; Geacintov, N. E.; Shafirovich, V. *J. Biol. Chem.* **2004**, *279*, 32106–32115.
- (21) Crean, C.; Geacintov, N. E.; Shafirovich, V. *Chem. Res. Toxicol.* **2008**, *21*, 358–373.
- (22) Lomoth, R.; Naumov, S.; Brede, O. *J. Phys. Chem. A* **1999**, *103*, 6571–6579.
- (23) Aravindakumar, C. T.; Schluchmann, M. N.; Rao, B. S. M.; von Sonntag, J.; von Sonntag, C. *Org. Biomol. Chem.* **2003**, *1*, 401–408.
- (24) von Sonntag, C.; Schuchmann, H.-P. *Angew. Chem., Int. Ed. Engl.* **1991**, *30*, 1229–1253.
- (25) Tallman, K. A.; Tronche, C.; Yoo, D. J.; Greenberg, M. M. *J. Am. Chem. Soc.* **1998**, *120*, 4903–4909.
- (26) Czapski, G.; Lymar, S. V.; Schwarz, H. A. *J. Phys. Chem. A* **1999**, *103*, 3447–3450.
- (27) Crean, C.; Geacintov, N. E.; Shafirovich, V. *J. Phys. Chem. B* **2009**, *113*, 12773–81.
- (28) McElroy, W. J. *J. Phys. Chem.* **1990**, *94*, 2435–2441.
- (29) Candeias, L. P.; Steenken, S. *J. Am. Chem. Soc.* **1993**, *115*, 2437–2440.
- (30) Candeias, L. P.; Steenken, S. *Chem.—Eur. J.* **2000**, *6*, 475–484.
- (31) Giese, B.; Spichty, M. *ChemPhysChem* **2000**, *1*, 195–198.
- (32) Kobayashi, K.; Tagawa, S. *J. Am. Chem. Soc.* **2003**, *125*, 10213–8.
- (33) Kobayashi, K.; Yamagami, R.; Tagawa, S. *J. Phys. Chem. B* **2008**, *112*, 10752–10757.
- (34) Steenken, S. *Chem. Rev.* **1989**, *89*, 503–520.
- (35) Bachler, V.; Hildenbrand, K. *Radiat. Phys. Chem.* **1992**, *40*, 59–68.
- (36) Adhikary, A.; Kumar, A.; Becker, D.; Sevilla, M. D. *J. Phys. Chem. B* **2006**, *110*, 24171–24180.
- (37) Knobloch, B.; Linert, W.; Sigel, H. *Proc. Natl. Acad. Sci. U.S.A.* **2005**, *102*, 7459–64.
- (38) Crean, C.; Geacintov, N. E.; Shafirovich, V. *Free Radicals Biol. Med.* **2008**, *45*, 1125–1134.
- (39) Perrier, S.; Hau, J.; Gasparutto, D.; Cadet, J.; Favier, A.; Ravanat, J. L. *J. Am. Chem. Soc.* **2006**, *128*, 5703–5710.
- (40) Misiaszek, R.; Crean, C.; Geacintov, N. E.; Shafirovich, V. *J. Am. Chem. Soc.* **2005**, *127*, 2191–2200.
- (41) Joffe, A.; Mock, S.; Yun, B. H.; Kolbanovskiy, A.; Geacintov, N. E.; Shafirovich, V. *Chem. Res. Toxicol.* **2003**, *16*, 966–973.